Inorganica Chimica Acta 445 (2016) 140–148

Contents lists available at ScienceDirect

Inorganica Chimica Acta

journal homepage: www.elsevier.com/locate/ica

Four new nickel(II) complexes based on an asymmetric Salamo-type ligand: Synthesis, structure, solvent effect and electrochemical property

Wen-Kui Dong *, Jian-Chun Ma, Li-Chun Zhu, Yang Zhang, Xia-Liang Li

School of Chemical and Biological Engineering, Lanzhou Jiaotong University, Lanzhou 730070, PR China

ARTICLE INFO

Article history:
Received 10 October 2015
Received in revised form 14 January 2016
Accepted 12 February 2016
Available online 2 March 2016

Keywords:
Asymmetric Salamo-type ligand
Ni(II) complex
Synthesis
Crystal structure
Electrochemical property

ABSTRACT

Four new solvent-induced Ni(II) complexes with chemical formulae {[NiL(MeOH)(μ-OAc)]$_2$Ni}·2MeOH (**1**), {[NiL(EtOH)(μ-OAc)]$_2$Ni} (**2**), {[NiL(i-PrOH)(μ-OAc)]$_2$Ni} (**3**) and {[NiL(DMF)(μ-OAc)]$_2$Ni}·2DMF·0.44H_2O (**4**), where H_2L = 5-methoxy-4′-chloro-2,2′-[(1,3-propylene)dioxybis(nitrilomethylidyne)]diphenol, have been synthesized and characterized by elemental analyses, ^{1}H NMR, FT–IR, UV–Vis spectra and X-ray crystallography. X-ray crystallographic analyses of the Ni(II) complexes reveal that they crystallize in the triclinic system, space group $P\bar{1}$, and consists of three Ni(II) ions, two deprotonated L^{2-} units, two μ-acetato ligands and two coordinated solvent molecules. In each of the Ni(II) complexes, the Ni(II) ions are hexa-coordinated with a slightly distorted octahedral coordination geometries. Although the molecule structures of the Ni(II) complexes are similar each other, obtained in different solvents, the supramolecular structures are entirely different. The complexes **1** and **3** possess a self-assembled infinite 2D and 1D supramolecular structures via the intermolecular hydrogen bonds, respectively. But the Ni(II) complexes **2** and **4** are formed 0D structures by intramolecular hydrogen bonds. Cyclic voltammetry is used to characterize electrochemical property of the Ni(II) complex **1**.

1. Introduction

N_2O_2 Salen-type ligands are easily obtained by the reaction of salicylaldehyde or its derivatives with diamines, coordinated to transition metal ions in a N_2O_2 tetradentate fashion to obtain stable mononuclear complexes [1,2]. In addition, there are a number of report on the synthesis of transition metal homometallic tri- and polynuclear complexes consisting of two or more molecules of Salen-type [3–6] or Salamo-type [7,8] ligands. In these complexes, μ_2-phenoxo bridging plays an important role in assembling transition metal ions and two ligands. Although transition metal complexes of Salen or its derivatives have been extensively studied in catalysts [9–12], nonlinear optical materials [13,14], magnetic materials [15–17], electrochemical conduct [18,19], and biological fields [20]. The novel structures of Salen-type complexes are also fascinating, which may lead to a better property.

In the recent years, a part of our research program concentrated on the syntheses of Salamo-type complexes by the structural motifs of substituent groups [21–26]. The structural motifs of complex molecules rest on several factors, such as the property of the central atoms, the performance of the ligands, the coordinated counter ions or small neutral molecules, the solvent systems and so on. When the same ligand is allowed to react with the same metal salt in different solvents with the same exterior conditions, the performance of the ligands, the coordinated small neutral molecules and the solvent systems often play important roles in the formation of the molecular structure of the complexes [7]. In order to study the electrochemical properties and further investigate solvent effect of Salamo-type complexes, we have designed and synthesized four solvent-induced Ni(II) complexes by the complexation of a N_2O_2 asymmetric Salamo-type ligand H_2L with Ni$(CH_3COO)_2$·4H_2O, under the same exterior conditions in four different solvents.

2. Experimental section

2.1. Materials and methods

5-Chlorosalicylaldehyde and 4-methoxybenzaldehyde of 98% purity have been used without further purification. 1,3-Dibromoprophane and other reagents were analytical grade reagents from Tianjin Chemical Reagent Factory.

C, H, and N analyses were obtained using a GmbH VarioEL V3.00 automatic elemental analysis instrument. Elemental analysis for Ni was detected by an IRIS ER/S·WP-1 ICP atomic emission spectrometer.

* Corresponding author. Tel.: +86 931 4938703; fax: +86 931 4956512.
E-mail address: dongwk@126.com (W.-K. Dong).

http://dx.doi.org/10.1016/j.ica.2016.02.043
0020-1693/

Melting points were obtained by the use of a microscopic melting point apparatus made in Beijing Taike Instrument Limited Company and were uncorrected. IR spectra were recorded on a VERTEX70 FT-IR spectrophotometer, with samples prepared as KBr (500–4000 cm^{-1}) and CsI (100–500 cm^{-1}) pellets. UV–Vis absorption spectra were recorded on a Shimadzu UV-2550 spectrometer. ^1H NMR spectra were determined by German Bruker AVANCE DRX-400 spectrometer. The electrochemical property was measured by the use of a PGSTAT128N Autolab.

2.2. Synthesis and characterization of H_2L

Major synthetic route of 5-methoxy-4′-chloro-2,2′-[(1,3-propylene)dioxybis(nitrilomethylidyne)]diphenol (H_2L) are given in Scheme 1. 1, 3-Bis(aminooxy)prophane was synthesized according to an analogous method reported earlier [27].

The N_2O_2 Salamo-type ligand H_2L was synthesized according a literature procedure [28]. A solution of 2-hydroxy-5-chlorobenzaldehyde *O*-(2-(aminooxy)ethyl) oxime (0.490 g, 2 mmol) in ethanol (10 mL) was added to a solution of 4-methoxybenzaldehyde (0.304 g, 2 mmol) in ethanol (10 mL). The mixture was stirred at 60 °C for 5 h. After cooling to room temperature, the precipitates were collected. The product was dried in vacuo, and a colorless flocculent solid was obtained. Yield, 0.462 g (61%). M.p. 108–109 °C. ^1H NMR (400 MHz, $CDCl_3$, δ, ppm): 2.13–2.16 (m, 2H, CH_2), 3.81 (s, 3H, CH_3), 4.26–4.32 (m, 4H, CH_2), 6.48 (dd, J = 16 Hz, 2H, ArH), 6.91 (d, J = 24 Hz, 1H, ArH), 7.04 (d, J = 28 Hz, 1H, ArH), 7.12 (d, J = 16 Hz, 1H, ArH), 7.22 (dd, J = 20 Hz, 1H, ArH), 8.12 (d, J = 8 Hz, 2H, CH=N), 9.82 (s, 1H, OH), 9.98 (s, 1H, OH). UV–Vis (ethanol): λ_{max} (ε_{max}) 274 and 311 nm (31300 and 20500 L M^{-1} cm^{-1}). IR (KBr, cm^{-1}) 3435(b), 3117(w), 2978(w), 2872(w), 1628(s), 1609(s), 1508(s), 1483(s), 1369(m), 1269(s), 1211(s). *Anal.* Calc. for $C_{18}H_{19}ClN_2O_5$: C, 57.07; H, 5.06, N; 7.40. Found: C, 57.13; H, 5.10,N; 7.49%.

2.3. Synthesis of the Ni(II) complexes **1**, **2**, **3** and **4**

Four solvent-induced Ni(II) complexes **1**, **2**, **3** and **4** are obtained by the reaction of Salamo-type ligand H_2L with $Ni(OAc)_2{\cdot}4H_2O$ in a 2:3 M ratio in mixed solution of acetone and methanol, ethanol, i-propanol or (methanol and DMF), respectively. The Ni(II) complex **4** also can be obtained by the reaction of the Ni(II) complexes **1**, **2** or **3** with DMF solvent, respectively. The single crystals of the Ni(II) complexes **1**, **2**, **3** and **4** suitable for X-ray diffraction analysis were obtained by solvent partially evaporated.

2.3.1. {[NiL(MeOH)(μ-OAc)]$_2$Ni}·2MeOH (**1**)

A methanol solution (3 ml) of $Ni(OAc)_2{\cdot}4H_2O$ (37.24 mg, 0.15 mmol) was added dropwise to a acetone solution (1 ml) of H_2L (37.88 mg, 0.1 mmol) at room temperature. The color of the mixed solution turned to pale green immediately. After stirring for 10 min at room temperature, the mixture was filtered and the filtrate was allowed to stand at room temperature for a week, the solvent partially evaporated and green block-like single crystals suitable for X-ray crystallographic analysis were obtained. Yield, 29.99 mg (51%). UV–Vis (ethanol): λ_{max} (ε_{max}) 246 and 352 nm (77800 and 26200 L M^{-1} cm^{-1}). IR (KBr, cm^{-1}) 3588(b), 2936(w), 1611(vs), 1539(s), 1420(s), 1301(s), 1213(s), 525(w), 475(w), 415(w). *Anal.* Calc. for {[NiL(MeOH)(μ-OAc)]$_2$Ni}·2MeOH ($C_{44}H_{56}Cl_2N_4Ni_3O_{18}$): C, 44.94; H, 4.80; N, 4.76; Ni, 14.97. Found: C, 44.73; H, 4.87; N, 4.61; Ni, 14.78%.

2.3.2. {[NiL(EtOH)(μ-OAc)]$_2$Ni} (**2**)

The single crystal of the Ni(II) complex **2** was obtained by a similar procedure, an ethanol solution (3 ml) of $Ni(OAc)_2{\cdot}4H_2O$ (3.72 mg, 0.015 mmol) was added dropwise to a acetone solution (1 ml) of H_2L (3.79 mg, 0.01 mmol). The pale green mixture was filtered and the filtrate was allowed to stand at room temperature for a week, the solvent partially evaporated and green block-like single crystals suitable for X-ray crystallographic analysis were obtained. Yield, 2.67 mg (47%). UV–Vis (ethanol): λ_{max} (ε_{max}) 246 and 352 nm (94700 and 30600 L M^{-1} cm^{-1}). IR (KBr, cm^{-1}) 3566(b), 2939(w), 1611(vs), 1535(s), 1420(s), 1300(s), 1215(s), 518(w), 473(w), 419(w). *Anal.* Calcd. for {[NiL(EtOH)(μ-OAc)]$_2$Ni} ($C_{44}H_{50}Cl_2N_4Ni_3O_{16}$): C, 46.44; H, 4.43; N, 4.92; Ni, 15.47. Found: C, 46.33; H, 4.48; N, 4.39; Ni, 15.32%.

2.3.3. {[NiL(i-PrOH)(μ-OAc)]$_2$Ni} (**3**)

The single crystal of the Ni(II) complex **3** was obtained by a similar procedure, an i-propanol solution (3 ml) of $Ni(OAc)_2{\cdot}4H_2O$ (3.72 mg, 0.015 mmol) was added dropwise to a acetone solution (1 ml) of H_2L (3.79 mg, 0.01 mmol). The pale green mixture was filtered and the filtrate was allowed to stand at room temperature for a week, the solvent partially evaporated and green block-like single crystals suitable for X-ray crystallographic analysis were obtained. Yield, 2.69 mg (46%). UV–Vis (ethanol): λ_{max} (ε_{max}) 246 and 352 nm (69,500 and 22,300 L M^{-1} cm^{-1}). IR (KBr, cm^{-1}) 3564(b), 2941(w), 2833(w), 1607(vs), 1537(s), 1422(s), 1301(s), 1217(s), 519(w), 475(w), 419(w). *Anal.* Calcd. for {[NiL(i-PrOH)(μ-OAc)]$_2$Ni} ($C_{46}H_{56}Cl_2N_4Ni_3O_{16}$): C, 47.30; H, 4.83; N, 4.80; Ni, 15.08. Found: C, 47.11; H, 4.90; N, 4.73; Ni, 14.90%.

2.3.4. {[NiL(DMF)(μ-OAc)]$_2$Ni}·2DMF·0.44H_2O (**4**)

The single crystal of the Ni(II) complex **4** was obtained by a similar procedure, a methanol solution (3 ml) of $Ni(OAc)_2{\cdot}4H_2O$ (3.72 mg, 0.015 mmol) was added dropwise to a mixture solution of acetone and DMF (1 ml) of H_2L (3.79 mg, 0.01 mmol). The pale green mixture was filtered and the filtrate was allowed to stand

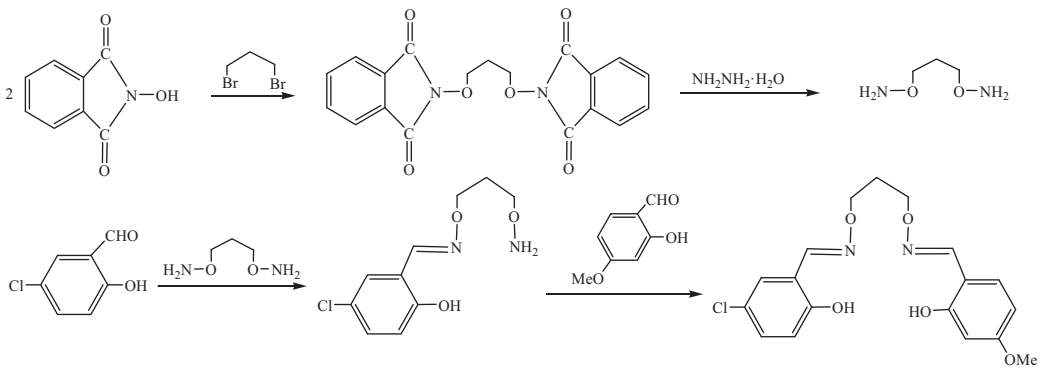

Scheme 1. The synthetic route of H_2L.

at room temperature for a week, the solvent partially evaporated and green block-like single crystals suitable for X-ray crystallographic analysis were obtained. Yield, 2.76 mg (41%). UV–Vis (ethanol): λ_{max} (ε_{max}) 246 and 352 nm (65 000 and 22 300 L M^{-1} cm^{-1}). IR (KBr, cm^{-1}) 3616(b), 2835(w), 1645(s), 1607(vs), 1537(s), 1472(s), 1422(s), 1300(s), 1217(s), 521(w), 476(w), 417 (w). *Anal.* Calc. for {[NiL(DMF)(μ-OAc)]$_2$Ni}·2DMF·0.44H_2O ($C_{52}H_{68.88}Cl_2N_8Ni_3O_{18.44}$): C, 46.33; H, 5.15; N, 8.31; Ni, 13.06. Found: C, 46.13; H, 5.29; N, 8.27; Ni, 12.98%.

2.4. Crystal structure determination

The single crystals of the Ni(II) complexes **1**, **2**, **3** and **4** with approximate dimensions of 0.19 × 0.23 × 0.25, 0.19 × 0.24 × 0.26, 0.23 × 0.25 × 0.31 and 0.17 × 0.18 × 0.22 mm were placed on a Bruker Smart diffractmeter equipped with Apex CCD area detector, respectively. The diffraction data were collected using a graphite monochromated Mo Kα radiation (λ = 0.71073 Å) at 293 (2), 296(2), 294.58(10) and 296(2) K, respectively. The structures were solved by using the program SHELXS-97 and Fourier difference techniques, and refined by full-matrix least-squares method on F^2 using SHELXL-97 [29]. Anisotropic thermal parameters were used for the nonhydrogen atoms and isotropic parameters for the hydrogen atoms. Hydrogen atoms were added geometrically and refined using a riding model. Crystallographic data and refinement for all of the Ni(II) complexes are summarized in Table 1.

2.5. Cyclic voltammetry

The electrochemical measurement was carried out at 25 °C in a standard three-electrode cell, consisting of a glassy carbon (GC) disc (Φ = 5 mm) as working electrode, a platinum wire as auxiliary and a Hg/HgO as reference. The sample was made of 1.0 × 10^{-3} M DMF solution with adding 0.1 M tetrabutylammonium perchlorate (TBAP) as supporting electrolyte. The potentials were recorded between −1.0 and +1.5 V at 100 mV s^{-1} scan rate.

3. Results and discussion

3.1. IR spectra analyses

IR spectra of H_2L and its corresponding Ni(II) complexes **1**, **2**, **3** and **4** are shown the characteristic C=N stretching band. The free ligand H_2L appears at 1609 cm^{-1}, while the C=N bands of the

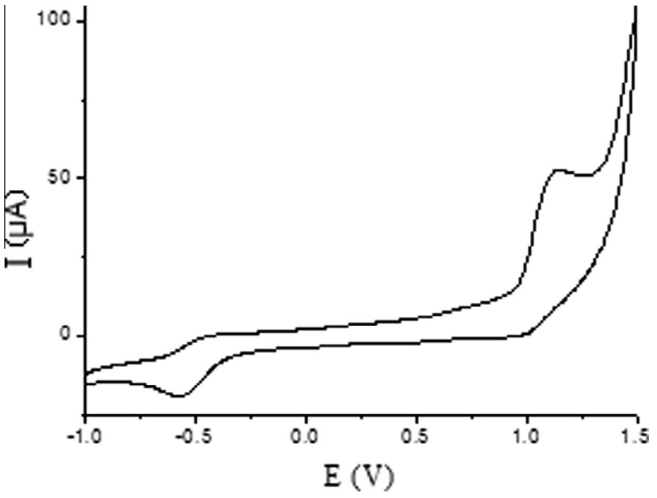

Fig. 1. Cyclic voltammetry of the Ni(II) complex **1** in DMF + TBAP 0.1 M at 100 mV s^{-1} scan rate on GC electrode at 25 °C.

Table 1
X-ray crystallographic data collection, solution and refinement parameters for the Ni(II) complexes **1**, **2**, **3** and **4**.

Compound code	**1**	**2**	**3**	**4**
Empirical formula	$C_{44}H_{56}Cl_2N_4Ni_3O_{18}$	$C_{44}H_{50}Cl_2N_4Ni_3O_{16}$	$C_{46}H_{56}Cl_2N_4Ni_3O_{16}$	$C_{52}H_{68.88}Cl_2N_8$ $Ni_3O_{18.44}$
Formula weight	1175.95	1137.91	1167.97	1348.10
T (K)	293(2)	296(2)	294.58(10)	296(2)
Wavelength (Å)	0.71073	0.71073	0.71073	0.71073
Crystal system	triclinic	triclinic	triclinic	triclinic
Space group	$P\bar{1}$	$P\bar{1}$	$P\bar{1}$	$P\bar{1}$
Unit cell dimensions				
a (Å)	9.585(4)	9.388(4)	10.893(3)	11.1521(14)
b (Å)	11.594(5)	12.479(6)	10.926(3)	11.8576(15)
c (Å)	12.634(5)	13.992(6)	12.438(3)	12.3578(16)
α (°)	69.802(6)	65.285(6)	103.25(2)	72.564(2)
β (°)	82.727(6)	82.914(7)	105.99(2)	76.515(2)
γ (°)	84.221(7)	68.341(6)	110.83(2)	76.383(2)
Cell volume (Å^3)	1304.6(9)	1383.0(11)	1238.7(7)	1491.8(3)
Z	1	1	1	1
D_{calc} (g cm^{-3})	1.497	1.366	1.566	1.500
μ (mm^{-1})	1.247	1.172	1.301	1.104
F(000)	610	588	606	702
Crystal size (mm)	0.19 × 0.23 × 0.25	0.19 × 0.24 × 0.26	0.23 × 0.25 × 0.31	0.17 × 0.18 × 0.22
θ Range (°)	1.7–25.5	1.9–25.0	3.3–26.0	1.8–27.8
Index ranges	$-11 \leqslant h \leqslant 11$, $-14 \leqslant k \leqslant 7$, $-15 \leqslant l \leqslant 14$	$-11 \leqslant h \leqslant 7$, $-14 \leqslant k \leqslant 14$, $-16 \leqslant l \leqslant 16$	$-13 \leqslant h \leqslant 13$, $-13 \leqslant k \leqslant 9$, $-15 \leqslant l \leqslant 15$	$-11 \leqslant h \leqslant 14$, $-9 \leqslant k \leqslant 15$, $-15 \leqslant l \leqslant 16$
Collected reflections	7382	9273	7888	9981
Unique reflections (R_{int})	4790 (0.018)	4740 (0.063)	4855 (0.095)	6882 (0.023)
Completeness (%) (θ)	98.9 (25.498)	97.2 (25.010)	99.2 (26.022)	97.7 (27.760)
Data/ restraints/parameters	4790/0/321	4740/210/316	4855/3/329	6882/9/392
Goodness-of-fit on (GOF) F^2	1.091	1.020	0.984	1.033
Final R_1 Indices [$I > 2\sigma(I)$]	R_1 = 0.0440, wR_2 = 0.1190	R_1 = 0.0822, wR_2 = 0.1965	R_1 = 0.0906, wR_2 = 0.1737	R_1 = 0.0509, wR_2 = 0.1284
R Indices (all data)	R_1 = 0.0600, wR_2 = 0.1268	R_1 = 0.1057, wR_2 = 0.2099	R_1 = 0.1700, wR_2 = 0.2286	R_1 = 0.0883, wR_2 = 0.1513
Residuals peak/hole (e/ Å^3)	1.14 and −0.38	1.30 and −0.71	1.28 and −0.82	0.82 and −0.84

Ni(II) complexes **1**, **2**, **3** and **4** are observed at 1611, 1611, 1607 and 1607 cm^{-1}, respectively. The shift of this C=N absorption by about 3 and 2 cm^{-1} on going from the free ligand H_2L to the Ni(II) complexes **1**, **2**, **3** and **4**.

The Ar–O stretching frequencies appear as a very strong band within 1269–1211 cm^{-1} range as reported for similar Salen-type ligands [30]. These bands occur at 1269 cm^{-1} for H_2L, 1213 cm^{-1} for the Ni(II) complex **1**, 1215 cm^{-1} for the Ni(II) complex **2** and 1217 cm^{-1} for the Ni(II) complexes **3** and **4**. The Ar–O stretching frequency is shifted to lower frequency, indicating that the Ni–O bonds are formed between the Ni(II) ions and oxygen atoms of phenolic groups [31]. In addition, the O–H stretching bands can be found at 3435 cm^{-1} in the free ligand H_2L and the broad absorption centered on 3588, 3566, 3564 and 3616 cm^{-1} in the Ni(II) complexes **1**, **2**, **3** and **4**, respectively, which are the evidence for the existence of alcohols or water molecules.

Table 2
Electrochemistry data (*vs* Hg/HgO) of the Ni(II) complex **1**.

	E_{pa} (V)	E_{pc} (V)	ΔE (V)	$E_{1/2}$ (V)	I_{pa} (μA)	I_{pc} (μA)	I_{pa}/I_{pc}
Ni(II)(salamo)/Ni (I)(salamo)	– 0.575	– 0.434	0.141	– 0.505	– 12.40	6.53	1.899
Ni(III)(salamo)/Ni (II)(salamo)	–	1.152	–	–	–	35.26	–

E_{pa} and E_{pc} are the anode and cathode electrode potential, respectively. $E_{1/2} = 1/2 (E_{pa} + E_{pc})$, $\Delta E = |E_{pa} - E_{pc}|$.

The far-infrared spectra of the Ni(II) complexes **1**, **2**, **3** and **4** are also obtained in the region 500–100 cm^{-1} in order to identify frequencies due to the Ni–O and Ni–N bonds. IR spectra of the Ni(II) complexes **1**, **2**, **3** and **4** show ν(Ni–N) (or ν(Ni–O)) vibrational absorption frequencies at 475, 473, 475 and 476 (or 415, 419, 419 and 417) cm^{-1}, respectively, which are consistent with the literature frequency values [32,33]. These bands are observed as new bands for the Ni(II) complexes **1**, **2**, **3** and **4** and are not present in the spectrum of the free ligand H_2L.

3.2. UV–Vis spectra analyses

The absorption spectra of H_2L and its corresponding Ni(II) complexes **1**, **2**, **3** and **4** in ethanol solution show that the spectra of the Ni(II) complexes **1**, **2**, **3** and **4** are similar to each other, but are different from the spectrum of the ligand H_2L. The UV–Vis spectrum of the free ligand H_2L exhibits two absorption peaks at *ca.* 274 and 311 nm. The absorption peak at 274 nm can be attributed to the π–π^* transition of the benzene rings and the absorption peak at 311 nm can be assigned to the intra-ligand π–π^* transition of the C=N bonds [34]. Compared with the absorption peak of the free ligand H_2L, a new absorption peak is observed at 352 nm in the Ni(II) complexes **1**, **2**, **3** and **4**, which are assigned to the n–π^* charge transfer transition from the filled pπ orbital of the bridging phenolic oxygen to the vacant d-orbital of the Ni(II) ions [35]. It is noteworthy that the same UV–Vis absorption spectra of the Ni(II)

Table 3
Selected bond lengths (Å) and bond angles (°) for the Ni(II) complexes **1**, **2**, **3** and **4**.

Complex **1**		Complex **2**		Complex **3**		Complex **4**	
Bond	Distance	Bond	Distance	Bond	Distance	Bond	Distance
Ni2–N1	2.109(3)	Ni2–N1	2.113(6)	Ni1–O1	2.018(6)	Ni2–N1	2.056(3)
Ni2–N2	2.124(3)	Ni2–N2	2.081(7)	Ni1–O4	1.991(5)	Ni2–N2	2.059(3)
Ni2–O3	2.031(2)	Ni2–O6	2.013(6)	Ni1–O6	2.199(6)	Ni2–O4	2.026(3)
Ni2–O4	2.045(2)	Ni2–O1	2.021(5)	Ni1–O7	2.040(6)	Ni2–O3	2.031(2)
Ni2–O7	2.033(2)	Ni2–O2	2.034(5)	Ni1–N1	2.076(7)	Ni2–O2	2.042(3)
Ni2–O9	2.110(3)	Ni2–O7	2.118(5)	Ni1–N2	2.047(7)	Ni2–O8	2.174(3)
Ni1–O3	2.075(2)	Ni1–O1	2.082(5)	Ni2–O1	2.101(6)	Ni1–O1	2.055(2)
Ni1–O4	2.104(2)	Ni1–O2	2.084(5)	Ni2–O4	2.071(5)	Ni1–O3	2.078(2)
Ni1–O6	2.129(2)	Ni1–O8	2.102(5)	Ni2–O8	2.023(5)	Ni1–O4	2.106(2)
Bond	Angle	Bond	Angle	Bond	Angle	Bond	Angle
O3–Ni1–O3$^{\#}$	180.0	O2–Ni1–O2	180.0	O1–Ni1–O6	88.9(2)	O1–Ni1–O1$^{\#}$	180.0
O3–Ni1–O4$^{\#}$	103.99(9)	O2–Ni1–O1$^{\#}$	102.80(19)	O1–Ni1–O7	93.1(2)	O1–Ni1–O3$^{\#}$	92.50(10)
O3–Ni1–O4	76.01(9)	O2–Ni1–O1	77.20(19)	O1–Ni1–N1	87.0(2)	O1–Ni1–O3	87.50(10)
O3–Ni1–O6$^{\#}$	89.01(9)	O1–Ni1–O1$^{\#}$	180.0	O1–Ni1–N2	167.9(2)	O3$^{\#}$–Ni1–O3	180.00(2)
O3–Ni1–O6	90.99(9)	O2–Ni1–O8	91.97(19)	O4–Ni1–O1	81.8(2)	O1–Ni1–O4$^{\#}$	89.82(10)
O4–Ni1–O4$^{\#}$	180.0	O1$^{\#}$–Ni1–O8	88.9(2)	O4–Ni1–O6	92.5(2)	O3$^{\#}$–Ni1–O4$^{\#}$	79.63(9)
O4–Ni1–O6$^{\#}$	89.01(9)	O1–Ni1–O8	91.1(2)	O4–Ni1–O7	90.5(2)	O3–Ni1–O4$^{\#}$	100.37(9)
O4–Ni1–O6	90.99(9)	O2–Ni1–O8$^{\#}$	88.03(19)	O4–Ni1–N1	168.3(2)	O1–Ni1–O4	90.18(10)
O4$^{\#}$–Ni1–O6	89.01(9)	O1–Ni1–O8$^{\#}$	88.9(2)	O4–Ni1–N2	87.3(3)	O3–Ni1–O4	79.63(9)
O6$^{\#}$–Ni1–O6	180.0	O8–Ni1–O8$^{\#}$	180.0	O7–Ni1–O6	176.5(2)	O4$^{\#}$–Ni1–O4	180.00(11)
N1–Ni2–N2	109.41(12)	O6–Ni2–O1	90.9(2)	O7–Ni1–N1	93.4(3)	O4–Ni2–O3	82.65(10)
N1–Ni2–O9	89.95(11)	O6–Ni2–O2	93.2(2)	O7–Ni1–N2	92.0(3)	O4–Ni2–O2	92.34(11)
O3–Ni2–N2	86.07(10)	O1–Ni2–O2	79.7(2)	N1–Ni1–O6	83.9(3)	O3–Ni2–O2	90.67(10)
O3–Ni2–O4	78.30(9)	O6–Ni2–N2	93.2(3)	N2–Ni1–O6	86.5(3)	O4–Ni2–N1	87.32(12)
O3$^{\#}$–Ni2–O7	92.52(10)	O1–Ni2–N2	86.2(2)	N2–Ni1–N1	103.6(3)	O3–Ni2–N1	168.90(13)
O3–Ni2–O9	90.64(10)	O2–Ni2–N2	164.6(2)	O1$^{\#}$–Ni2–O1	180.0	O2–Ni2–N1	94.49(12)
O4–Ni2–N1	86.23(10)	O6–Ni2–N1	88.9(2)	O4–Ni2–O1$^{\#}$	102.0(2)	O4–Ni2–N2	168.61(11)
O4–Ni2–N2	164.11(10)	O1–Ni2–N1	166.2(2)	O4–Ni2–O1	78.0(2)	O3–Ni2–N2	86.67(11)
O4–Ni2–O9	90.59(11)	O2–Ni2–N1	86.5(2)	O4$^{\#}$–Ni2–O4	180.0	O2–Ni2–N2	91.71(12)
O7$^{\#}$–Ni2–N1	88.05(11)	N2–Ni2–N1	107.7(3)	O8–Ni2–O1$^{\#}$	91.0(2)	N1–Ni2–N2	102.97(13)
O7$^{\#}$–Ni2–N2	89.53(11)	O6–Ni2–O7	176.0(2)	O8–Ni2–O1	89.0(2)	O4–Ni2–O8	91.41(10)
O7$^{\#}$–Ni2–O4	93.92(10)	O1–Ni2–O7	92.9(2)	O8–Ni2–O4$^{\#}$	91.3(2)	O3–Ni2–O8	90.00(10)
O7$^{\#}$–Ni2–O9	174.94(10)	O2–Ni2–O7	86.4(2)	O8–Ni2–O4	88.7(2)	O2–Ni2–O8	176.24(11)
O9–Ni2–N2	86.74(12)	N2–Ni2–O7	88.2(2)	O8$^{\#}$–Ni2–O8	180.0	N1–Ni2–O8	85.49(11)
O3–Ni2–N1	164.52(11)	N1–Ni2–O7	87.1(2)	O8$^{\#}$–Ni2–O4$^{\#}$	88.7(2)	N2–Ni2–O8	84.63(12)

Symmetry transformations used to generate equivalent atoms: $^{\#1}$: 1 − *x*, 1 − *y*, −*z*, $^{\#2}$: 1 − *x*, −*y*, 1 − *z*, $^{\#3}$: −*x*, 1−*y*, 1 − *z* and $^{\#4}$: 2 − *x*, 2 − *y*, 1 − *z* for the Ni(II) complexes **1**, **2**, **3** and **4**, respectively.

Table 4
Intra- and inter-molecular hydrogen geometries (Å, °) for the Ni(II) complexes **1**, **2**, **3** and **4**.

Complex	D–H	d(D–H)	d(H···A)	d(D···A)	∠DHA	A	Symmetry codes
1	O9–H9	0.86	1.76	2.605(4)	169	O10	*x*, *y*, −1 + *z*
	O10–H10	0.82	1.90	2.715(4)	171	O6	*x*, *y*, 1 + *z*
	C8–H8A	0.97	2.47	2.857(6)	103	O2	
	C10–H10	0.97	2.43	3.329(6)	154	O7	1 − *x*, 1 − *y*, −*z*
	C10–H10B	0.97	2.56	3.474(6)	158	O10	1 + *x*, *y*, −1 + *z*
	C16–H16	0.93	2.51	3.201(5)	132	O6	
2	C2–H2	0.93	2.59	3.276(10)	131	O8	
	C8–H8A	0.97	2.53	2.879(14)	101	O3	
	C10–H10A	0.97	2.56	2.895(13)	100	O4	
	C10–H10A	0.97	2.43	3.346(11)	157	O6	
	C16–H16	0.93	2.55	3.154(11)	123	O8	
	C16–H16	0.93	2.54	3.269(10)	135	O2	1 − *x*, −*y*, 1−*z*
3	O6–H6	0.86	2.17	3.010(8)	166	O2	−*x*, 1 − *y*, −*z*
	C2–H2	0.93	2.53	3.141(11)	124	O8	−*x*, 1−*y*, 1−*z*
	C5–H5	0.93	2.50	3.228(11)	135	O3	−*x*, 1 − *y*, −*z*
	C8–H8B	0.97	2.37	3.251(12)	151	O7	
	C14–H14	0.93	2.56	3.259(11)	132	O1	−x, 1 − i, 1−*z*
	C14–H14	0.93	2.57	3.189(11)	124	O8	−*x*, 1−*y*, 1−*z*
4	C8–H8A	0.97	2.52	3.323(5)	140	O2	
	C10–H10B	0.91	2.51	3.277(6)	142	O2	
	C16–H16	0.93	2.60	3.171(6)	120	O1	2 − *x*, 2−*y*, 1−*z*
	C20–H20	0.93	2.43	3.344(5)	168	O1	2−*x*, 2−*y*, 1−*z*
	C21–H21A	0.96	2.34	2.759(7)	106	O8	

complexes **1**, **2**, **3** and **4** clearly indicate that the structures of the four Ni(II) complexes are similar to each other.

3.3. Cyclic voltammetry

Fig. 1 shows cyclic voltammograms (CVs) of the Ni(II) complex **1** in DMF. The electrochemistry data (*vs* Hg/HgO) of the Ni(II) complex **1** are shown in Table 2. It is easy to see that the plots of the Ni(II) complex **1** exhibiting two redox pairs. The first anodic/cathodic couple potentials (E_{pa} = −0.575, E_{pc} = −0.434) is attributed to the Ni(II)(salamo)/Ni(I)(salamo) process (Ni(II)(salamo) + e ↔ Ni(I)(salamo)) [36]. The ratio of anodic to cathodic peak currents, I_{pa}/I_{pc} = 1.899 (I_{pa} = −12.40, I_{pc} = 6.53) and $\Delta E = |E_{pa} - E_{pc}|$ = 0.141 V, in agreement with a quasi-reversible electron-transfer process [37]. The second couple potentials is attributed to the Ni(II/I)(salamo) process, but the anodic peak is not observed, indicating a irreversible redox process. The cathodic peak potential is observed at E_{pc} = 1.152 V which corresponded to the process Ni(III)(salamo) + e → Ni(II)(salamo) [38]. In this system, the Ni(II)(salamo) complex is more stable than the Ni(III)(salamo) one.

3.4. Description of the crystal structures

Selected bond lengths (Å) and bond angles (°) are presented in Table 3. Hydrogen bonds in the Ni(II) complexes **1**, **2**, **3** and **4** are given in Table 4.

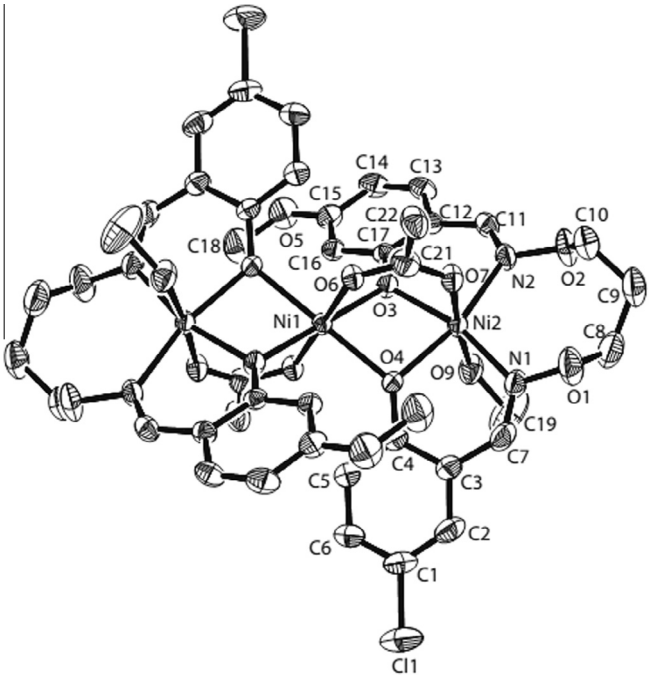

Fig. 2. Crystal structure of the Ni(II) complex **1**. The hydrogen atoms and solvent molecules are omitted for clarity.

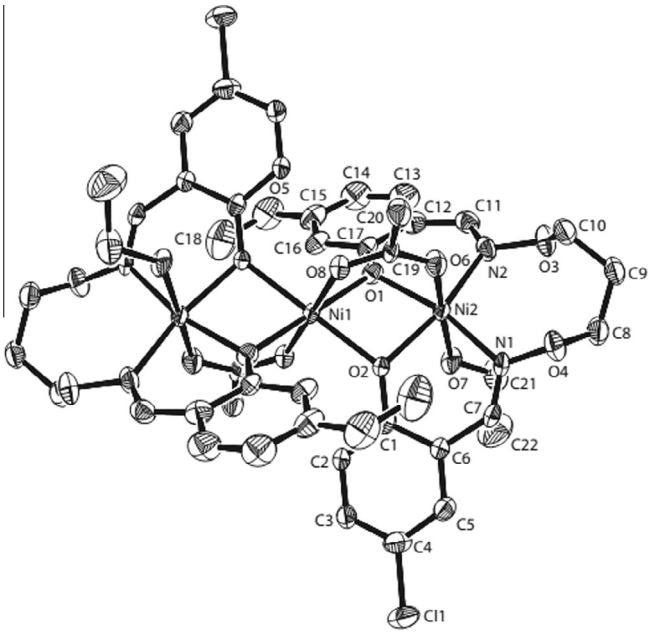

Fig. 3. Crystal structure of the Ni(II) complex **2**. The hydrogen atoms are omitted for clarity.

*3.4.1. Structure of the Ni(II) complex **1***

X-ray crystallographic analysis of the Ni(II) complex **1** reveals a symmetric trinuclear structure. It crystallizes in the triclinic system, space group $P\bar{1}$, and consists of three Ni(II) ions, two L^{2-} units, two μ-acetato ligands, two coordinated methanol and two non-coordinated methanol molecules. Selected bond lengths and angles are listed in Table 3.

As shown in Fig. 2, the two terminal Ni(II) ions (Ni2 and Ni2$^{\#1}$) are both located in the cis-N_2O_2 coordination cavity of the deprotonated L^{2-} units, and carboxylate oxygen atom O7 from the μ-acetato bridge and oxygen atom O9 from the methanol ligand, coordinated to Ni2 in axial positions. The dihedral angle between the coordination planes of N1–Ni2–O4 and N2–Ni2–O3 is 2.81 (2)°, indicating slight distortion octahedral geometry from the square planar structure. Because Ni2 and Ni2$^{\#1}$ are symmetry related, they have identical geometries. In addition, the coordination sphere of the central Ni(II) ions (Ni1) is completed by quadruple four μ-phenoxo oxygen atoms from two L^{2-} moieties and two μ-acetato oxygen atoms which adopt a familiar μ–O–C–O fashion. All of the six oxygen atoms coordinate to Ni1 constituting an octahedral geometry: one μ-acetato ligand serves as bridging group for Ni1 and Ni2 and another coordinates to Ni1 and Ni2$^{\#1}$, in both cases via Ni–O–C–O–Ni bridges. The bond angles of O7–Ni2–O9 (or O7$^{\#1}$–Ni2$^{\#1}$–O9$^{\#1}$) is 174.94(10)°, while the bond angles of O6–Ni1–O6$^{\#1}$ is 180.0°, showing that the center Ni(II) has a lower distortion than the terminal Ni(II) in octahedral coordination geometry. Thus, all the hexa-coordinated Ni(II) ions of the Ni(II) complex **1** have a slightly distorted octahedral coordination polyhedron. Furthermore, the distances of Ni1 and Ni2 (or Ni2$^{\#1}$) atoms to the six donors are in the range of 2.031(2)–2.129(2) Å. The distance of Ni1···Ni2 is 3.134(3) Å, indicating weak inter-metal interaction, which is significantly longer than all of the Ni–O and Ni–N bonds. The Ni–N bonds (2.109(3) and 2.124(3) Å) around the terminal Ni(II) (Ni2 and Ni2$^{\#1}$) ions are slightly longer than Ni–O bonds (2.031(2) and 2.045(2) Å).

*3.4.2. Structure of the Ni(II) complexes **2**, **3** and **4***

X-ray crystal structure analyses of the Ni(II) complexes **2**, **3** and **4** reveal that the structures of the Ni(II) complexes **2**, **3** and **4** are similar to the Ni(II) complex **1**. The Ni(II) complexes **2**, **3** and **4** crystallize in the triclinic system, space group $P\bar{1}$, and consists of three Ni(II) ions, two L^{2-} units, two μ-acetato ligands, two coordinated solvent molecules (The solvent molecules are ethanol, i-propanol and DMF in the Ni(II) complexes **2**, **3** and **4**, respectively) and non-coordinated solvent molecules (two H_2O and one DMF in the Ni(II) complex **4**). All the hexa-coordinated Ni(II) ions of the Ni(II) complexes **2**, **3** and **4** have a slightly distorted octahedral coordination polyhedron. Crystal structures are shown in Figs. 3–5, respectively.

In the Ni(II) complexes **2**, **3** and **4**, all the terminal Ni(II) ions lie in a hexa-coordinated environment and adopt slightly distorted octahedral coordination geometry, where the inner N_2O_2 cavities of the pentadentate L^{2-} units as the basal planes, and two oxygen atoms from the coordinated solvent molecules (ethanol, i-propanol and DMF, respectively) occupies the axial positions. The primary bond lengths (Ni–O and Ni–N) of the Ni(II) complexes **2**, **3** and **4** are listed in Table 3. The dihedral angle between the two coordination planes of N1–Ni2–O2 and N2–Ni2–O19 (N1–Ni1–O1 and N2–Ni1–O4 or N1–Ni2–O4 and N2–Ni2–O3) is 6.07(2) in the Ni(II) complex **2** (6.46(2) or 6.58(2)° in the Ni(II) complex **3** or **4**, respectively), which are larger than the Ni(II) complex **1**, showing that the terminal Ni(II) ions have a higher distortion than the Ni(II) complex **1** in octahedral geometry. The central Ni(II) ions are hexa-coordinated, surrounded by six oxygen atoms from the two [NiL(solvent)] units and two oxygen atoms from μ-acetato ligands, with the same coordination environment as that of the central Ni(II) ion in the Ni(II) complex **1**. Two phenoxo oxygen atoms bridge the terminal and central Ni(II) ions with a separation of 3.108(2), 3.067(2) and 3.063(2) Å in the Ni(II) complexes **2**, **3** and **4**, respectively, which are not sufficiently short to imply strong inter-metal bonding interaction.

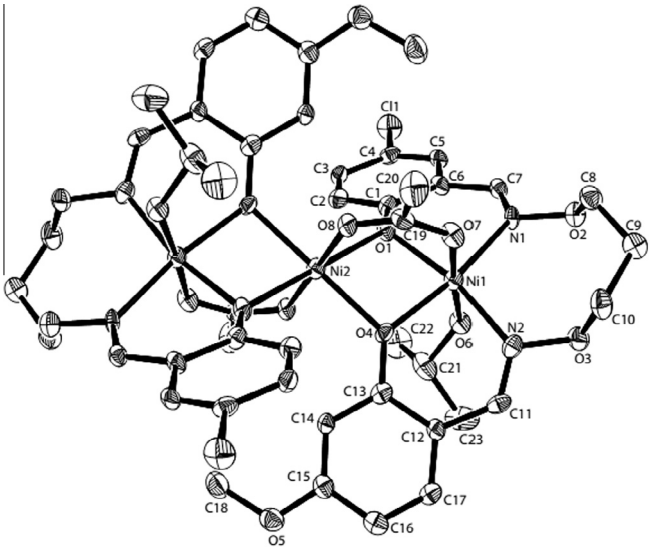

Fig. 4. Crystal structure of the Ni(II) complex **3**. The hydrogen atoms are omitted for clarity.

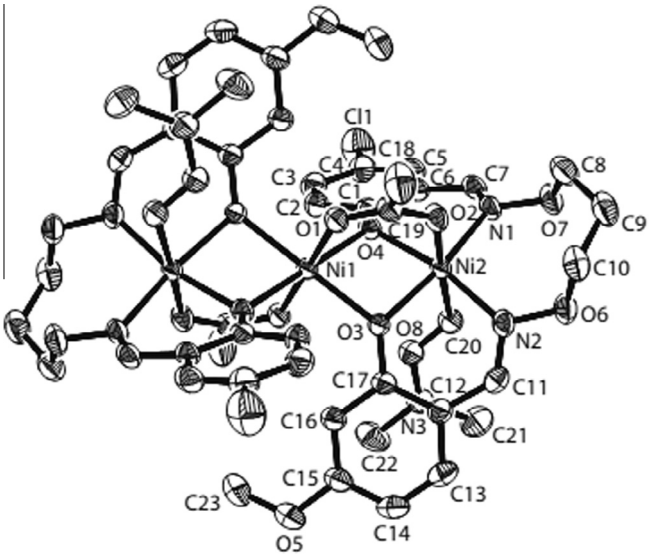

Fig. 5. Crystal structure of the Ni(II) complex **4**. The hydrogen atoms and solvent molecules are omitted for clarity.

*3.4.3. Supramolecular interaction of the Ni(II) complexes **1**, **2**, **3** and **4***

The molecular structures of four solvent-induced Ni(II) complexes **1**, **2**, **3** and **4** are similar each other, but the supramolecular structures are entirely different owed to the inter- and intramolecular hydrogen bonds (Table 4). In the crystal structure of the Ni(II) complex **1**, there are three pairs of intramolecular hydrogen bonding (C8–H8A···O2, C10–H10A···O7 and C16–H16···O6) and three pairs of intermolecular hydrogen bonding (O9–H9···O10, O10–H10···O6 and C10–H10B···O10) interactions. The oxygen (O10) atoms of the non-coordinated methanol molecules are hydrogen-bonded to the C10–H18B groups of another complex molecule,

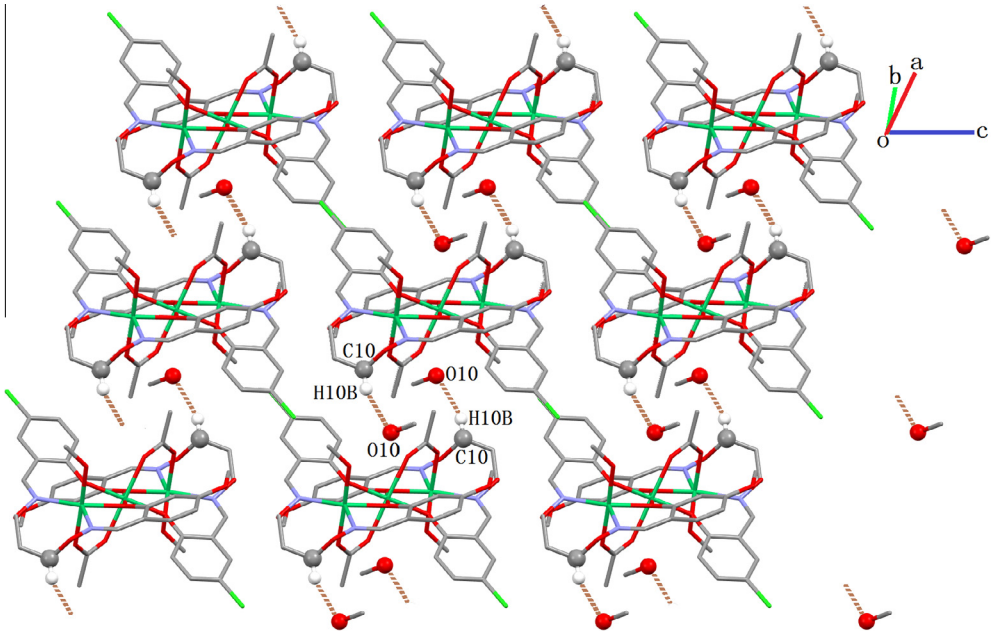

Fig. 6. Infinite 2D supramolecular structure of the Ni(II) complex **1** showing inter-molecular hydrogen bonds.

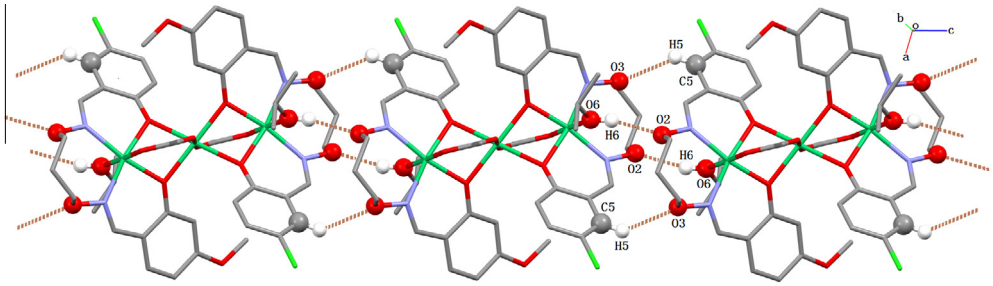

Fig. 7. Infinite 1D supramolecular structure of the Ni(II) complex **3** showing inter-molecular hydrogen bonds.

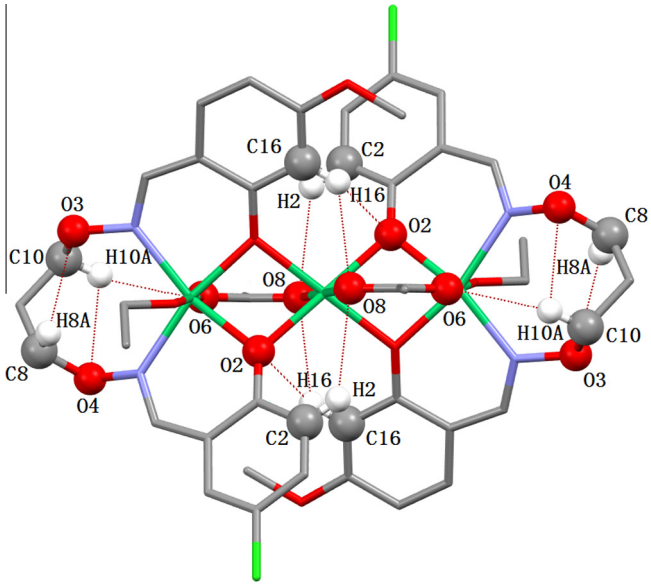

Fig. 8. 0D structure of the Ni(II) complex **2** showing intra-molecular hydrogen bonds.

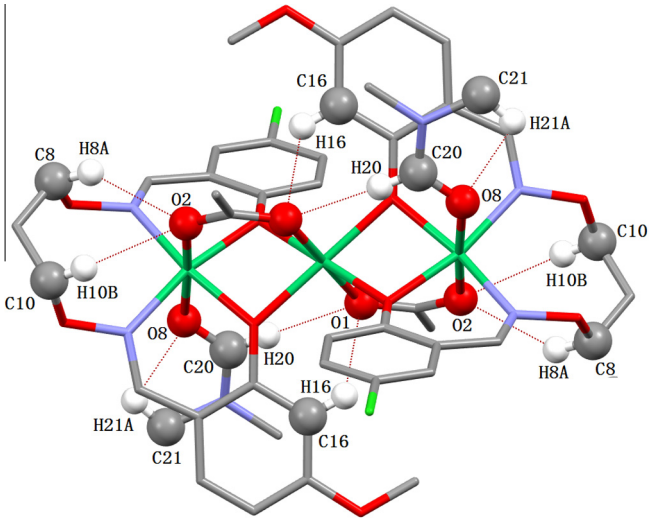

Fig. 9. 0D structure of the Ni(II) complex **4** showing intra-molecular hydrogen bonds.

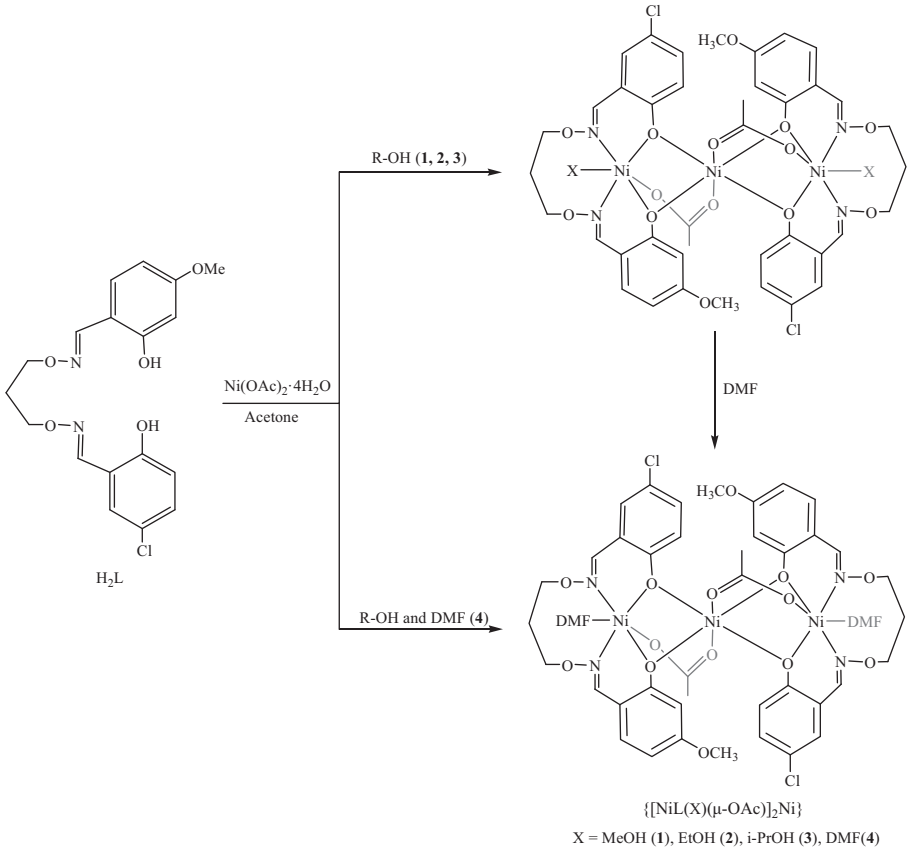

Scheme 2. Controlled design of the solvent-induced Ni(II) complexes **1**, **2**, **3** and **4**.

linking adjacent complex molecules into a infinite 2D supramolecular structure (Fig. 6).

There are four pairs of intramolecular hydrogen bonds and two pairs of intermolecular hydrogen bonds (Table 4) existing in the Ni(II) complex **3**. The Ni(II) complex **3** is further linked by a pairs of intermolecular C5–H5···O3 hydrogen bonding interactions between the –CH group of the O-alkyl chain and the aromatic rings of L^{2-} unit and a pairs of intermolecular O6–H6···O2 hydrogen bonding interactions between the –CH group of the O-alkyl chain and the coordinated i-propanol molecule to form a 1D infinite chain (Fig. 7).

However, there are not intermolecular hydrogen bonds in the Ni(II) complexes **2** and **4** which are stabilized by six and five pairs of intramolecular hydrogen bonding interactions (Table 4), respectively, forming a 0D isolated molecular structures (Figs. 8 and 9).

3.4.4. Solvent effect

As shown in Scheme 2, controlled design of the solvent-induced Ni(II) complexes **1**, **2**, **3** and **4**. Because of the coordination with different solvents (methanol, ethanol, i-propanol and DMF), the Ni(II) complexes **1**, **2**, **3** and **4** present two kinds of synthetic route: all the four Ni(II) complexes could been synthesized by the reaction of the Salamo-type ligand H_2L with $Ni(CH_3COO)_2{\cdot}4H_2O$ in different solvents. The Ni(II) complex **4** also could been synthesized by the Ni(II) complexes **1**, **2** or **3** dissolved in DMF solvent, because of the strong polarity and coordination ability of DMF which could displace the coordinated alcohol molecules of the Ni(II) complexes **1**, **2** or **3**. Although the molecule structures of the Ni(II) complexes are similar each other, obtained in different mixture solutions, the supramolecular structures are entirely different. The Ni(II) complexes **1** and **3** possess a self-assembling infinite 2D and 1D supramolecular structures via the intermolecular hydrogen bonds, respectively. But the Ni(II) complexes **2** and **4** form 0D isolated structures by intramolecular hydrogen bonds.

The influence of solvent effect is clearly revealed in selected bond distances (Å) and bond angles (°) for the Ni(II) complexes 1, 2, 3 and 4 (Table 3). It is noteworthy that the bond lengths from the oxygen atoms (O9, O7 and O6) of coordinated solvent molecules (methanol, ethanol or i-propanol) to the terminal Ni(II) ions in the Ni(II) complexes 1, 2 and 3 are 2.110(3), 2.118(5) and 2.199(6) Å, respectively, which present a regular elongation when the steric hindrance successively becomes larger from methanol, ethanol to i-propanol.

4. Conclusions

We have designed and synthesized four solvent-induced trinuclear Ni(II) complexes **1**, **2**, **3** and **4** with an asymmetric N_2O_2 Salamo-type ligand. X-ray crystal structure analyses of the Ni(II) complexes reveal that the structures of the Ni(II) complexes **1**, **2**, **3** and **4** are similar each other. They all form symmetric trinuclear structure with three Ni(II) ions, two L^{2-} units, two μ-acetato ligands and two coordinated solvent molecules. All the hexa-coordinated Ni(II) ions of the Ni(II) complexes **1**, **2**, **3** and **4** have a slightly distorted octahedral coordination polyhedron. Significantly, these Ni(II) complexes possess similar structures, but the supramolecular structures are entirely different. The Ni(II) complexes **1** and **3** possess a self-assembling infinite 2D and 1D supramolecular structure via the intermolecular hydrogen bonds, respectively. But the Ni(II) complexes **2** and **4** are formed 0D isolated structures by intramolecular hydrogen bonds. Cyclic voltammetry is used to characterize electrochemical properties of the Ni(II) complex **1**. The cyclic voltammograms of the Ni(II) complex **1**

exhibits two redox pairs. There is a quasi-reversible electron-transfer process which is found at anodic peak $E_{pa} = -0.575$ V. But the anodic peak is not observed at $E_{pc} = 1.152$ V, indicating a irreversible redox process.

Acknowledgements

This work was supported by the National Natural Science Foundation of China (21361015) and Graduate Student Guidance Team Building Fund of Lanzhou Jiaotong University (260001), which are gratefully acknowledged.

Appendix A. Supplementary material

CCDC 1421304, 1421305, 1421306 and 1421307 contain the supplementary crystallographic data for the Ni(II) complexes **1**, **2**, **3** and **4**. These data can be obtained free of charge from The Cambridge Crystallographic Data Centre via www.ccdc.cam.ac.uk/data_request/cif. Supplementary data associated with this article can be found, in the online version, at http://dx.doi.org/10.1016/j.ica.2016.02.043.

References

[1] L.Q. Ding, S.R. Liang, J.T. Zhang, C.F. Ding, Y. Chen, X.Q. Lü, Inorg. Chem. Commun. 44 (2014) 173.
[2] N. Zhang, C.Y. Huang, D.H. Shi, Z.L. You, Inorg. Chem. Commun. 14 (2011) 1636.
[3] C.D. Ene, S. Nastase, C. Maxim, A.M. Madalan, F. Tuna, M. Andruh, Inorg. Chim. Acta 363 (2010) 4247.
[4] A. Gutiérrez, M.F. Perpiñán, A.E. Sánchez, M.C. Torralba, M.R. Torres, Inorg. Chim. Acta 363 (2010) 1837.
[5] I. Cacelli, L. Carbonaro, P. La Pegna, Eur. J. Inorg. Chem. (2002) 1703.
[6] C.N. Chen, D.G. Huang, X.F. Zhang, F. Chen, H.P. Zhu, Q.T. Liu, C.X. Zhang, D.Z. Liao, L.C. Li, L.C. Sun, Inorg. Chem. 42 (2003) 3540.
[7] W.K. Dong, X.N. He, H.B. Yan, Z.W. Lv, X. Chen, C.Y. Zhao, X.L. Tang, Polyhedron 28 (2009) 1419.
[8] S. Akine, W.K. Dong, T. Nabeshima, Inorg. Chem. 45 (2006) 4677.
[9] C. Baleizão, H. Garcia, Chem. Rev. 106 (2006) 3987.
[10] D.J. Darensbourg, Chem. Rev. 107 (2007) 2388.
[11] P.G. Cozzi, Chem. Soc. Rev. 33 (2004) 410.
[12] R. Ziessel, Coord. Chem. Rev. 216 (2001) 195.
[13] S.D. Bella, I. Fragalà, Synth. Met. 115 (2000) 191.
[14] P.G. Lacroix, Eur. J. Inorg. Chem. 2001 (2) (2001) 339.
[15] S.S. Sun, C.L. Stern, S.T. Nguyen, J.T. Hupp, J. Am. Chem. Soc. 126 (2004) 6314.
[16] J.P. Costes, F. Dahan, A. Dupuis, Inorg. Chem. 39 (2000) 165.
[17] C. Edder, C. Piguet, J.C.G. Bünzli, G. Hopfgartner, Chem. Eur. J. 7 (2001) 3014.
[18] S. Kal, A.S. Filatov, P.H. Dinolfo, Inorg. Chem. 53 (2014) 7137.
[19] H.T. Shi, Y.G. Yin, Inorg. Chim. Acta 421 (2014) 446.
[20] P.G. Lacroix, Eur. J. Inorg. Chem. 2001 (2001) 339.
[21] L. Xu, Y.P. Zhang, Y.X. Sun, J.Y. Shi, W.K. Dong, Chin. J. Inorg. Chem. 23 (2007) 1999.
[22] W.K. Dong, X. Chen, Y.X. Sun, X.N. He, Z.W. Lv, H.B. Yan, X.L. Tang, C.Y. Zhao, Chin. J. Inorg. Chem. 24 (2008) 1325.
[23] W.K. Dong, X.N. He, Y.H. Guan, L. Xu, Z.L. Ren, Acta Cryst. E64 (2008) 1810.
[24] W.K. Dong, Y.X. Sun, Y.P. Zhang, L. Li, X.N. He, X.L. Tang, Inorg. Chim. Acta 362 (2009) 117.
[25] W.K. Dong, Y.X. Sun, C.Y. Zhao, X.Y. Dong, L. Xu, Polyhedron 29 (2010) 2087.
[26] W.K. Dong, Y.X. Sun, X.N. He, J.F. Tong, J.C. Wu, Spectrochim. Acta A 76 (2010) 476.
[27] S. Akine, T. Taniguchi, T. Nabeshima, Chem. Lett. 30 (2001) 682.
[28] S. Akine, T. Taniguchi, W.K. Dong, S. Masubuchi, T. Nabeshima, J. Org. Chem. 70 (2005) 1704.
[29] G.M. Sheldrick, SHELXS-97 and SHELXL-97, Fortran Programs for Crystal Structure Solution and Refinement, University of Gottingen, Gottingen, 1997.
[30] M. Eddaoudi, D.B. Moler, H. Li, B. Chen, T.M. Reineke, M. O'Keeffe, O.M. Yaghi, Acc. Chem. Res. 34 (2001) 319.
[31] W.K. Dong, G.H. Liu, Y.X. Sun, X.Y. Dong, X.H. Gao, Z. Naturforsch. 67b (2012) 17.
[32] H.F. Xu, S.H. Zhang, Y.M. Jiang, X.X. Zhong, F. Gao, Chin. J. Struct. Chem. 23 (2004) 808.
[33] A. Majumder, G.M. Rosair, A. Mallick, N. Chattopadhyay, S. Mitra, Polyhedron 25 (2006) 1753.
[34] T. Ghosh, B. Mondal, T. Ghosh, M. Sutradhar, G. Mukherjee, M.G.B. Drew, Inorg. Chim. Acta 360 (2007) 1753.
[35] S. Akine, Y. Morita, F. Utsuno, T. Nabeshima, Inorg. Chem. 48 (2009) 10670.
[36] I.C. Santos, M. Vilas-Boas, M.F.M. Piedade, C. Freire, M.T. Duarte, B. de Castro, Polyhedron 19 (2000) 655.
[37] A.J. Bard, L.R. Faulkner, Electrochemical Methods, Fundamentals and Applications, Wiley, New York, 2001.
[38] G.D. Munno, D. Armentano, T. Poerio, M. Julve, J.A. Real, J. Chem. Soc., Dalton Trans. (1997) 1813.